J. Chem. Sci. (2020)132:121
https://doi.org/10.1007/s12039-020-01821-1
© Indian Academy of Sciences

REGULAR ARTICLE

Cyclic zinc organophosphate based expanded ditopic *N,N′*-metalloligands

GULZAR A BHAT and RAMASWAMY MURUGAVEL*
Department of Chemistry, Indian Institute of Technology Bombay, Mumbai 400 076, India
E-mail: rmv@chem.iitb.ac.in

MS received 20 April 2020; revised 23 May 2020; accepted 5 June 2020

Abstract. A new series of zinc phosphate based novel elongated ditopic *N,N′*-metalloligands **[**Zn(X-dipp)(pyterpy)]$_2$·2MeOH (X= H (**1**), Cl (**2**), Br (**3**), I (**4**)], exemplifying expanded 4,4′-bipyridine spacer family, has been prepared by reacting 4′-(4″-pyridyl)-2,2′:6′,2″-terpyridine (pyterpy), 2,6-diisopropylphenyl phosphate (dippH$_2$) or its para-halo functionalized derivatives X-dippH$_2$ (X = Cl, Br, I) with Zn(OAc)$_2$.2H$_2$O in a mixture of solvents at room temperature. The formation of these metalloligands has been confirmed by their spectroscopic and analytical data. Solution and solid-state stability of these complexes have been confirmed by both mass spectroscopy and thermogravimetric analysis. The solid-state structures of **1–4** have further been established by single crystal X-ray diffraction studies, revealing that the *N,N′*-distance in these systems can be expanded approximately to 23 Å, as against the 7 Å separation observed for 4,4'-bipyridine. Compounds **2–4,** which contain two pyridyl nitrogen centers and two C–X functionalities that are orthogonal to each other, could offer new possibilities in their use as metalloligand to build extended 2-D and 3-D solids.

Keywords. Pyridyl terpyridine; metalloligands; halo functionalization; X-ray structures; spacer ligands.

1. Introduction

Metallophosphates are extensively investigated for their diverse applications in the fields of molecular sieves,[1] ion exchangers and adsorbents,[2] to size and shape selective catalysts and catalytic supports,[3] matrices for electronic and optical devices,[4] medicinal diagnosis[5] and gas storage materials.[6] During the last few decades, various forms of low-density, porous metallophosphates and phosphonates have been synthesized and characterized.[7] Metallophosphates are known to exist mostly as extended frameworks rather than discrete molecules.[8] Discrete or molecular metallophosphates besides being fundamental in understanding the mechanism of zeolite formation via a bottom up approach, also finds applications in mimicking naturally occurring enzymes like hydrolases, phosphatases, nucleases, etc.[7a,9] Rational synthetic routes to discrete metallophosphates have not been well established in the literature, but the available empirical results suggest that nuclearity of these compounds can be tuned by altering the reaction conditions and ancillary ligands employed.[10]

Two different synthetic approaches have been used in the literature so far to develop discrete metallophosphates, namely (i) use of chelating ancillary ligands which blocks polymerization of molecular phosphates and (ii) substitution of one or two hydroxyl groups of phosphoric acid by ester (–OR) linkages to reduce the reactivity and hence tendency to form extended metallophosphates.[11] In our laboratory, we have employed lipophilic phosphate esters, such as di-*tert*-butyl phosphate (dtbp-H) and 2,6-diisopropylphenyl phosphate (dippH$_2$) for the successful isolation of different SBUs of zeolites ranging from D4R, D6R to D8R, often offering insights into the mechanism of formation of naturally occurring zeolites.[7a,12]

In recent literature, the tridentate chelating ligand 4′-(4″-pyridyl)-2,2′:6′,2″-terpyridine (pyterpy) has been widely employed to generate transition metal complexes ranging from discrete molecules to polymers.[13] Pyterpy-based transition metal complexes

*For correspondence

Electronic supplementary material: The online version of this article (https://doi.org/10.1007/s12039-020-01821-1) contains supplementary material, which is available to authorized users.

Published online: 08 September 2020

having free pendant pyridyl sites were explored as expanded 4,4′-bipyridines in which N···N distance of the pendant 4-pyridyl donors is increased from ~7 Å to ~18 Å (Figure 1).[14] The pendant sites react with protons,[14b,15] alkylating agents[15] and transition metal ion, thus retaining their reactivity.[16] We have employed different N donor co-ligands along with $dippH_2$ and isolated a multitude of compounds, many of which either highlight or mimic the mechanism of zeolite formation.[7a,9d,12b,17] We have also recently reported on phosphate and pytpy bridged dimeric and polymeric copper phosphates whose DNA cleavage and cytotoxicity activities are of significance.[18] We have also reported on dimeric manganese, cobalt, and nickel phosphates with 4′-chloro-2,2′:6′,2″-terpyridine (Cl-terpy) as ancillary ligand and investigated their catalytic activity in alcohol oxidation reactions.[19] In this context, the present contribution deals with the use of tridentate chelating ligand pyterpy and para-halo functionalized phosphates [(X-$dippH_2$) for isolating metalloligands with phosphate-containing cyclic core, and N···N distance between the two pendant 4-pyridyl donors is increased to 23 Å as depicted in Figure 1.

2. Experimental

2.1 *Materials, methods and instruments*

All the reactions were carried out under the ambient conditions inside a fume hood without any further precaution to exclude air and moisture. Melting points were measured in glass capillaries and are reported uncorrected. Infrared spectra were obtained on a Perkin–Elmer Spectrum One FTIR spectrometer as KBr diluted discs. Microanalyses were performed on a Thermo Finnigan (FLASH EA 1112) microanalyzer. Thermogravimetric analyses were carried out on a Perkin–Elmer Pyris thermal analysis system under a stream of nitrogen gas at a heating rate of 10°C/min. The ESI-MS studies were carried out on Bruker MaXis Impact Mass Spectrometer. Solvents were purified according to the standard procedures prior to their immediate use. Commercially available starting materials such as $Zn(OAc)_2.2H_2O$ (S.D. Fine), 2,6-diisopropyl phenol (Sigma Aldrich), 2-acetyl pyridine (Sigma Aldrich), 4-pyridine carboxyaldehyde (Sigma Aldrich), and ammonium acetate (spectrochem) were used as procured. Compounds such as 4′-(4‴-pyridyl)-2,2′:6′,2″-terpyridine(pyterpy),[20] 2,6-isopropylphenyl-phosphate($dippH_2$),[21] 4-chloro-, 4-bromo- and 4-iodo-2,6-diisopropylphenyl phosphates (X-$dippH_2$),[22] were synthesized according to the methods previously reported in literature.

2.2 *Synthesis of **1–4***

2.2.1 *Synthesis of **1***: To a solution of $Zn(OAc)_2.H_2O$ (43 mg, 0.20 mmol) in 10 mL of methanol, the mixture of pyterpy (62 mg, 0.20 mmol) and $dippH_2$ (51 mg, 0.20 mmol) in $CHCl_3/CH_3CN$(1:1 v/v) was added with constant stirring at room temperature. The solution was stirred for 3 h, filtered and kept for crystallization. Colorless crystals of **40** were obtained in a couple of days. Yield: 54%; Mp: > 250°C; Anal. Calc. for $C_{68}H_{78}N_8P_2O_{12}Zn_2$ (Mw = 1388) Found (Calc.): C, 59.07(58.56); H, 5.43(5.07); N, 5.86(8.34). FTIR (as KBr disc, cm^{-1}): 3663 (vs), 3432 (br), 2961 (s) 1596 (s), 1468 (s), 1253 (s), 1179 (s), 1090 (s), 989 (vs), 896 (s), 795 (s), 538 (s).[31] P NMR (solid state, 202 MHz, ppm) δ: –1.74 ppm. ESI-MS Calcd. for $C_{64}H_{62}N_8O_8P_2Zn_2$(M+H): *m/z* 1265 found *m/z* 1265.

2.2.2 *Synthesis of **2***: To a solution of $Zn(OAc)_2.2H_2O$ (43 mg, 0.20 mmol) in 10 mL of methanol, a mixture of pyterpy (62 mg, 0.20 mmol) and Cl-$dippH_2$ (58 mg, 0.20 mmol) in $CHCl_3/CH_3CN$(1:1 v/v) was added with constant stirring and the clear solution obtained was stirred at room temperature, filtered and kept for crystallization. In a couple of days, colorless crystals were obtained. Yield 64%. Mp > 250°C; Anal. Calc. for $C_{66}H_{70}N_8Cl_2P_2O_{10}Zn_2$ Found (Calc.): C, 55.32 (56.67), H, 4.73 (5.04), N, 7.90 (8.01), FT-IR (as KBr disc, cm^{-1}): 3677 (vs), 3184(br), 2944 (s), 1595 (s), 1426 (s), 1253 (s), 1190 (s), 1075 (s), 1000 (s), 896 (s), 795 (s), 538 (s). ESI-MS Calcd. for $C_{64}H_{62}N_8O_8P_2Cl_2Zn_2$(M+H): *m/z* 1333 found *m/z* 1333.

2.2.3 *Synthesis of **3***: To a solution of $Zn(OAc)_2.2H_2O$ (43 mg, 0.20 mmol) in 10 mL of methanol a mixture of pyterpy (62 mg, 0.20 mmol) and Br-$dippH_2$ (67 mg, 0.20 mmol) in $CHCl_3/CH_3CN$ (1:1 v/v) was added with constant stirring. The clear solution obtained was stirred at room temperature for 3 h, after which the mixture was filtered and kept for crystallization. In a couple of days colorless crystals were obtained. Yield: 56 %; Mp: > 250°C; Anal. Calc. for $C_{66}H_{70}N_8Br_2P_2O_{10}Zn_2$ Found (Calc.): C, 51.86 (53.28), H, 4.55 (4.74), N, 7.53 (7.53). FT-IR (as KBr disc, cm^{-1}): 3419 (br), 2926 (vs), 2865 (s), 1619 (s), 1595 (s), 1425 (s), 1189 (s), 1000(s),(s), 873 (s), 794 (s), 538 (s). ESI-MS Calcd. for $C_{64}H_{62}N_8O_8P_2Br_2Zn_2$(M+H): *m/z* 1421 found *m/z* 1421.

2.2.4 *Synthesis of **4***: To a solution of $Zn(OAc)_2.2H_2O$ (43 mg, 0.20 mmol) in 10 mL of methanol, a mixture

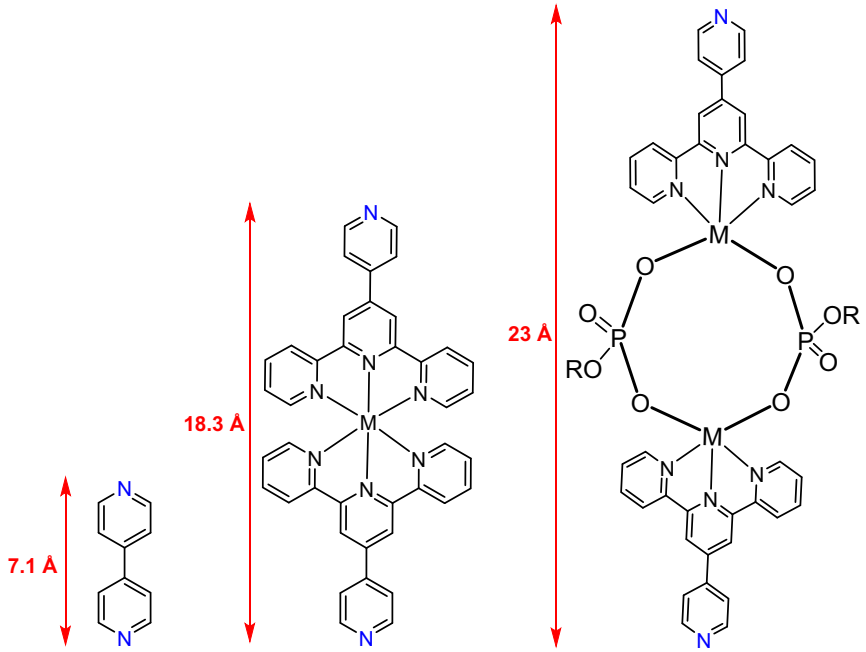

Figure 1. Comparison of N···N distances of expanded 4,4′-bipyridine metalloligands.

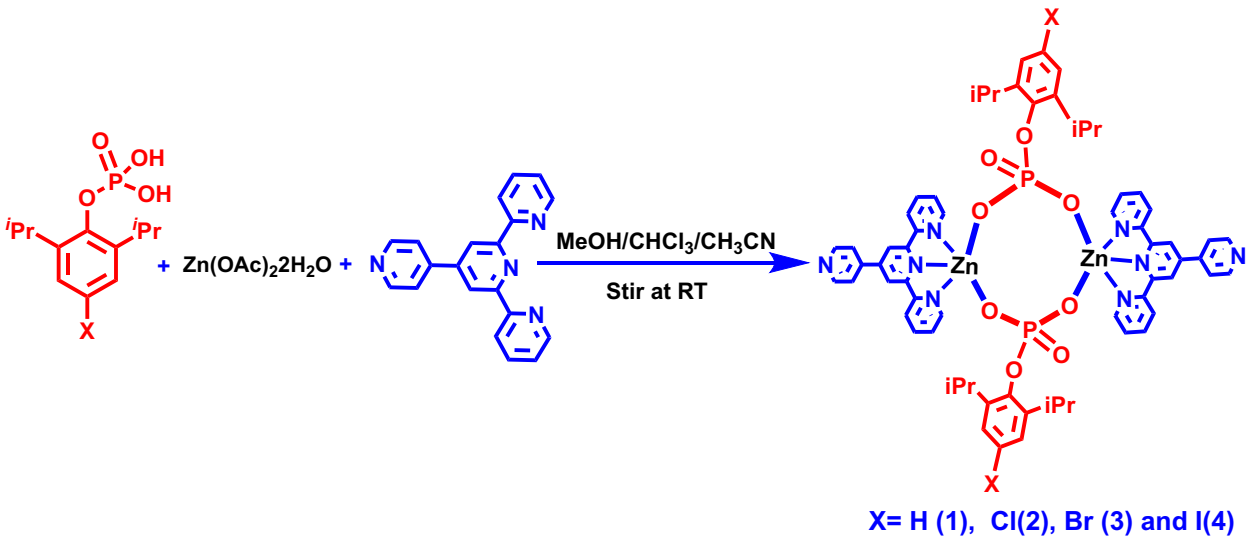

Scheme 1. Synthesis of **1–4**.

of pyterpy (62 mg, 0.20 mmol) and I-dippH$_2$ (76 mg, 0.20 mmol) in $CHCl_3/CH_3CN$ (1:1 v/v) was added with constant stirring and the resulting clear solution was stirred at room temperature for 2 h, filtered and kept for crystallization. In a couple of days, colorless crystals were obtained. Yield: 53%; Mp: > 250°C. Anal. Calc. for $C_{67}H_{71}Cl_3N_8I_2P_2O_{10}Zn_2$ Found (Calc.): C, 48.29 (47.30), H, 4.55 (4.21), N, 7.00 (6.59). FTIR (as KBr disc, cm^{-1}): 3419 (br), 2926 (vs), 2865 (s), 1619 (s), 1595 (s), 1425 (s), 1189 (s), 1000 (s),(s), 873 (s), 794 (s), 538 (s). ESI-MS Calcd. For $C_{64}H_{60}I_2N_8O_8P_2Zn_2$ (M+H): *m/z* 1515 found *m/z* 1515.

2.3 *X-ray crystallography*

Single crystal x-ray diffraction data were collected on a Rigaku Saturn 724+ CCD diffractometer with a Mo-Kα radiation source (λ = 0.71075 Å) at 150 K. Rigaku *Crystal Clear-SM Expert* software was used for data

Table 1. Crystallographic data and refinement details for compounds **1–4**.

Compound	1	2	3	4
CCDC number	1996512	1996513	1996514	1996515
Empirical formula	$C_{68}H_{78}N_8O_{12}P_2Zn_2$	$C_{68}H_{76}Cl_2N_8O_{12}P_2Zn_2$	$C_{68}H_{76}Br_2N_8O_{12}P_2Zn_2$	$C_{68}H_{76}I_2N_8O_{12}P_2Zn_2$
FW	1392.06	1460.94	1549.86	1946.66
Temp (K)	150(2)	150(2) K	130(2) K	130(2) K
Crystal system	Triclinic	Triclinic	Triclinic	Triclinic
Space group	*P* -1	*P* -1	*P* -1	*P* -1
a (Å)	11.519(3)	11.725(7)	11.762(3)	11.267(3)
b (Å)	13.345(3)	13.272(8)	13.243(3)	13.376(3)
c (Å)	13.422(3)	13.609(8)	13.609(8)	13.797(3)
α (°)	115.082(3)	114.901(4)	114.573(3)	83.971(8)
β (°)	108.5900(10)	113.608(4)	114.165(3)	87.234(7)
γ (°)	97.934(2)	94.520(5)	93.423(2)	88.975(7)
V [Å^3]	1679.1(7)	1680.3(17)	1704.5(8)	2065.2(8)
Z	1	1	1	1
D(calcd), [mg/cm^3]	1.377	1.444	1.510	1.422
μ [mm^{-1}]	0.829	0.909	1.990	1.625
Θ range (°)	2.829 to 24.999	2.872 to 24.995	2.860 to 24.995	3.262 to 24.997
No. of reflns. collected	12362	12676	12615	15549
Independent reflns	5842	5860	5940	7193 (0.0338)
GOF	1.054	1.111	1.047	1.066
R1($I_0 > 2\sigma(I_0)$)	0.0312	0.0670	0.0392	0.0771
wR2 (all data)	0.0842	0.1429	0.1047	0.2070

collection. Data integration and indexing were performed with the *CrysAlisPro* software suite. *WinGX* module was used to perform all the calculations.[23] The structures were solved by direct methods (*SIR-92*).[24] The final structure refinement was carried out using full-least-squares methods on F^2 using *SHELXL-2014*.[25] All non-hydrogen atoms were refined anisotropically. The hydrogen atoms were refined isotropically as rigid atoms in their idealized locations. Crystal data and structure refinement details for **1–4** are given in Table 1.

3. Results and Discussion

3.1 *Synthesis and characterization of **1–4***

An equimolar reaction of $Zn(OAc)_2.H_2O$ with X-dippH_2 (X = H, Cl, Br and I) and pyterpy in MeOH/$CHCl_3$/CH_3CN (1:1:1 v/v) under ambient conditions yielded a colorless solution. The reaction mixture after being stirred for a few minutes was filtered and kept undisturbed to yield $[Zn_2(X\text{-dipp})_2(pyterpy)_2].2MeOH$ [X = H (**1**); X = Cl (**2**); X = Br (**3**) and X = I (**4**)] as colorless crystals within one week (Scheme 1). The yields of single crystals obtained for products **1–4** were in the range of 53–64% (see Experimental).

Compounds **1–4** are stable under ambient conditions and have been characterized by various spectroscopic and analytical methods. The absence of any peaks around 2300 cm^{-1} clearly indicates complete deprotonation of the aryl phosphates. In addition, the compounds show sharp absorption bands at 1180, 1089, 988 cm^{-1} for **1;** 1164, 1037, 997 cm^{-1} for **2**; 1161, 1074, 1003 cm^{-1} for **3;** and 1188, 1118, 1000 cm^{-1} for **4** due to the P = O stretching and M−O−P asymmetric and symmetric stretching vibrations (Figure S1, Supplementary Information). Presence of broad resonances in the CP-MAS ^{31}P NMR spectra at δ –1.67, –1.64, –1.82 and –4.03 ppm for **1–4**, respectively, implies the presence of a single type of phosphorus center in these compounds (Figure S2, Supplementary Information). The existence of compounds **1–4** in solution state as dimers with free pendant nitrogen centers were further confirmed by ESI-MS. Acetonitrile solutions of these compounds show molecular ion peaks whose experimental and simulated isotopic pattern are in good agreement with each other (Figure 2 and Figures S3–S5, Supplementary Information). Microanalytical data obtained from crystalline products **1–4** further establish their elemental composition as well as purity.

Thermal decomposition characteristics of molecular zinc phosphates have been studied by the authors[26] and Don Tilley and co-workers[27] some years ago as a possible source for the preparation of ceramic zinc pyro and metaphosphates. Accordingly, thermal decomposition studies of compounds **1–4** were also

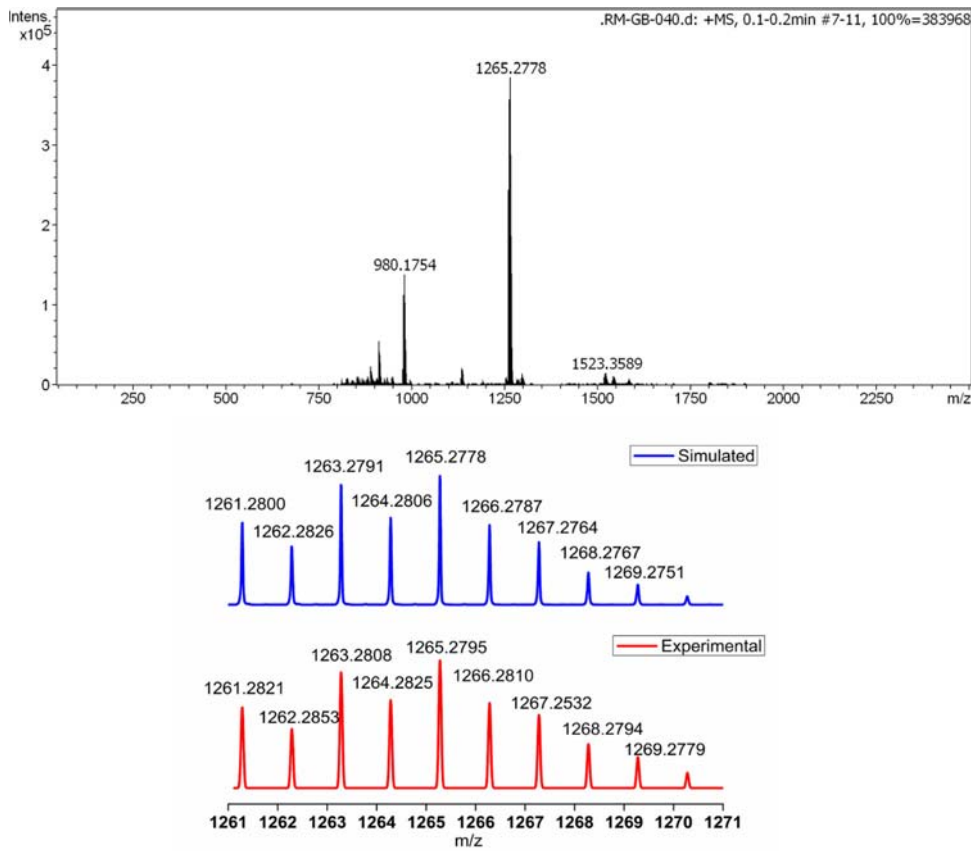

Figure 2. (Top) ESI-MS spectrum of **1** (positive ion mode) showing $[M+H]^+$ peak at *m/z* 1265.27; (bottom) selected portion of ESI-MS spectrum of **1** showing good agreement between simulated and experimental isotopic pattern of $[M+H]^+$ peak.

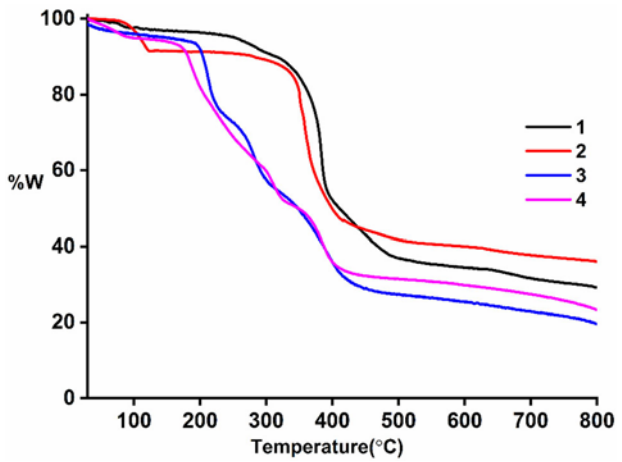

Figure 3. TGA plots of **1–4** at heating rate of 10°C/min under N_2.

carried out under the flow of N_2 at a heating rate of 10°C/min. The thermograms of all the compounds reveal an initial weight loss of 4–6% due to lattice solvent molecules. On further increasing the temperature, loss of organic moieties like aryl substituents of phosphate and pyridine groups of pyterpy ligand occurs leading to the formation of $Zn_2P_2O_7$ as shown in Figure 3.

3.2 *Molecular structures of **1–4***

Colorless, needle-shaped crystals of compounds **1–4** were grown from mixture of $CH_3CN/CHCl_3/CH_3OH$ (1:1:1 v/v) solvents (optimized for maximum solubility of the reagents employed) at room temperature. All the four compounds are isostructural and crystallize in the centrosymmetric triclinic space group *P*-1. A perspective view of the molecular structures of **1–4** are shown in Figure 4. Due to the isostructural nature of **1–4,** only the molecular structure of **1** is discussed in detail (compounds **2–4** exhibit similar structural features). The asymmetric part of the unit cell in **1** consists one-half of the molecule of **1,** with one Zn(II) ion, one pyterpy ligand, and one doubly deprotonated $dippH_2$ phosphate ligand besides one lattice methanol molecule. In the dimeric structure, the two metal ions are bridged by two phosphate ligands to form a $Zn_2P_2O_4$ eight-membered cyclic core. Apart from the

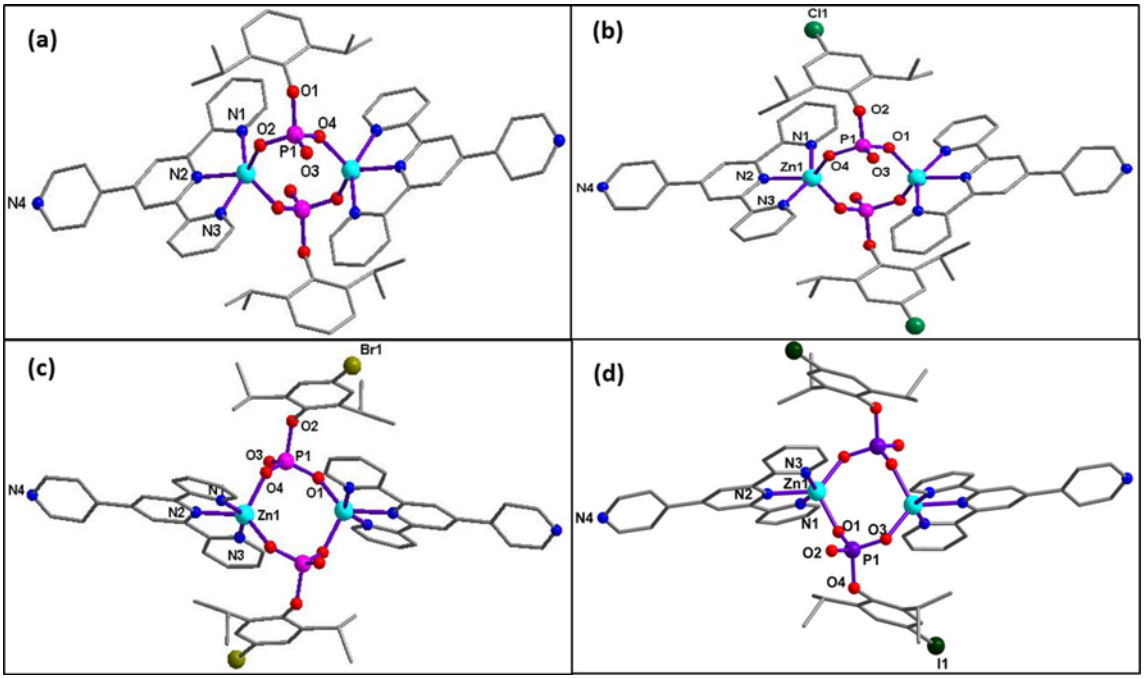

Figure 4. (a) Molecular structure of **1**. Selected bond distances and angles for **1**: Zn(1)-N(1) 2.1754 (2), Zn(1)-N(2) 2.0974(2), Zn(1)-N(3) 2.1964(2), Zn(1)-O(2) 1.9352(2), Zn(1)-O(4) 1.9261(2), N4-N4′ 22.26 Å; N(2)-Zn(1)-N(1) 74.87(6), N(2)-Zn(1)-N(3) 74.69(6), O(4)-Zn(1)-N(3) 94.80(6), O(2)-Zn(1)-N(2) 125.71(6), O(4)-Zn(1)-O(2) 116.28(6)°. (b) Molecular structure of **2**. Selected bond distances and angles for **2**: Zn(1)-N(1) 2.170(4), Zn(1)-N(2) 2.099(4), Zn(1)-N(3) 2.181(4), Zn(1)-O(1) 1.929(3), Zn(1)-O(4) 1.931(3) N4-N4′ 22.37 Å, N(2)-Zn(1)-N(1) 74.58(2), N(2)-Zn(1)-N(3) 74.45(2), O(4)-Zn(1)-N(3) 91.06(14), O(1)-Zn(1)-N(3) 96.94(2), O(4)-Zn(1)-O(1) 115.88(2)°. (c) Molecular structure of **3**. Selected bond distances and angles for **3**: Zn(1)-N(1) 2.196(2), Zn(1)-N(2) 2.107(2), Zn(1)-N(3) 2.175(2), Zn(1)-O(1) 1.9300(2), Zn(1)-O(4) 1.940(2), N4-N4′ 22.33 Å; N(2)-Zn(1)-N(1) 74.32(9), N(2)-Zn(1)-N(3) 74.68(9), O(1)-Zn(1)-N(1) 90.45(9), O(4)-Zn(1)-N(1) 98.93(9), O(4)-Zn(1)-O(2) 114.52(9)°. (d) Molecular structure of **4**. Selected bond distances and angles for **4**: Zn(1)-N(1) 2.189(5), Zn(1)-N(2) 2.101(5), Zn(1)-N(3) 2.174(5), Zn(1)-O(1) 1.934(4), Zn(1)-O(3) 1.940(4), N4-N4′ 22.23 Å; N(2)-Zn(1)-N(1) 74.50(2), N(2)-Zn(1)-N(3) 74.94(2), O(1)-Zn(1)-N(1) 94.90(2), O(3)-Zn(1)-N(2) 130.64(2), O(1)-Zn(1)-O(3) 113.67(2)°. Hydrogen atoms and lattice solvent molecules are omitted for clarity in all four compounds.

phosphate bridges, each zinc ion is chelated by a tridentate pyterpy ligand, making the metal to be pentacoordinate, whose coordination geometry can best be described as distorted square pyramidal and also as confirmed by shape analysis, where we got least energy for this geometry (see ESI for shape analysis data). In this geometry, the basal plane is occupied by pyterpy ligand and oxygen atom from a phosphate anion whereas the fifth coordination site is occupied by oxygen of the second phosphate ligand.

The distances between the two metal ions is 4.22 Å, whereas the two phosphorus atoms are 4.78 Å apart. The central Zn(1)–N(2) pyterpy bond (2.099(4) Å) is slightly shorter than the peripheral Zn(1)–N(1) and Zn(1)–N(3) bonds [(2.170(4) and 2.181(4) Å, respectively], as has been observed in many chelating terpyridine complexes.[28] The Zn(1)–O(1) and Zn(1)–O(4) bond distances, (1.929(3) and 1.931(3) Å, respectively), are comparable to literature reported values for zinc phosphates.[29] The most important structural feature in **1–4** is the significantly long distance between the pendant pyridyl nitrogen donor atoms (N4…N4' 22.40 Å). To the best of our knowledge, this is the longest reported distance between the donor atoms in any ditopic spacer ligand.

4. Conclusions

Four new dinuclear zincophosphates can be isolated as single crystals by reacting 2,6-diisopropylphenyl phosphate or its halo functionalized derivatives with 4′-(4″-pyridyl)-2,2′:6′,2″-terpyridine co-ligand and zinc acetate. All the four compounds have been characterized by various spectroscopic and analytic techniques and molecular structures were established by single crystal X-ray diffraction studies. These dimeric compounds have eight-membered ring as the central core, resembling the S4R building units of zeolites and have uncoordinated pendant pyridyl coordination sites which makes them expanded metalloligands with N···N distances which are as large as

~23 Å. These novel metalloligands may exhibit interesting coordination chemistry which can be potentially used as spacer ligands in preparing heterometallic MOF systems. We are currently investigating these possibilities.

Supplementary Information (SI)

FT-IR, NMR and ESI MS spectra and the result of SHAPE analysis are available as supplementary information. CCDC 1996512 (**1**), 1996513 (**2**), 1996514 (**3**) and 1996515 (**4**) contain the supplementary crystallographic data for this paper. Supplementary Information is available at www.ias.ac.in/chemsci.

Acknowledgements

This work was supported by an EMR grant of SERB, New Delhi (EMR/2017/002767) and J. C. Bose Fellowship grant (SB/S2/JCB-85/2014). GAB thank UGC, New Delhi for research fellowship.

References

1. (a) Singha D K, Mahata P 2015 Highly selective and sensitive luminescence turn-on-based sensing of Al^{3+} ions in aqueous medium using a MOF with free functional sites. *Inorg. chem.* **54** 6373; (b) Lee J, Farha O K, Roberts J, Scheidt K A, Nguyen S T, Hupp J T 2009 Metal–organic framework materials as catalysts. *Chem. Soc. Rev.* **38** 1450; (c) Sculley J P, Zhou H C 2012 Enhancing amine-supported materials for ambient air capture. *Angew. Chem. Int.* **51** 12660; (d) Li H-Y, Wei Y-L, Dong X-Y, Zang S-Q, Mak T C 2015 Novel Tb-MOF embedded with viologen species for multi-photofunctionality: Photochromism, photomodulated fluorescence, and luminescent pH sensing. *Chem. Mater.* **27** 1327
2. (a) Kandori K, Nakashima H, Ishikawa T 1993 Inner structure of uniform spherical metal phosphate particles: II. Nickel phosphate. *J. Colloid Interface Sci.* **160** 499; (b) Li X S, Courtney A R, Yantasee W, Mattigod S V, Fryxell G E 2006 Templated synthesis of mesoporous titanium phosphates for the sequestration of radionuclides. *Inorg. Chem. Commun.* **9** 293; (c) Katz H, Scheller G 1991 Polar orientation of dyes in robust multilayers by zirconium phosphate-phosphonate interlayers. *Science* **254** 1485; (d) Bhaumik A, Inagaki S 2001 Mesoporous titanium phosphate molecular sieves with ion-exchange capacity. *J. Am. Chem. Soc.* **123** 691; (e) Shah B, Chudasam U 2012 Application of zirconium phosphonate—a novel hybrid material as an ion exchanger. *Desalin. Water Treat.* **38** 276; (f) Alvarez C, Llavona R, Garcia J R, Suarez M, Rodriguez J 1987 Lamellar inorganic ion exchangers. Hydrogen(1+)/calcium(2+) ion exchange in. gamma.-titanium phosphate. *Inorg. Chem.* **26** 1045
3. (a) Lin R, Ding Y, Gong L, Dong W, Wang J, Zhang T 2010 Efficient and stable silica-supported iron phosphate catalysts for oxidative bromination of methane. *J. Catal.* **272** 65; (b) Wang Y, Wang X, Su Z, Guo Q, Tang Q, Zhang Q, Wan H 2004 SBA-15-supported iron phosphate catalyst for partial oxidation of methane to formaldehyde. *Catal. today* **93** 155; (c) Muneyama E, Kunishige A, Ohdan K, Ai M 1996 Reduction and reoxidation of iron phosphate and its catalytic activity for oxidative dehydrogenation of isobutyric acid. *J. Catal.* **158** 378; (d) Ma T-Y, Zhang X-J, Yuan Z-Y 2009 Hierarchically meso-/macroporous titanium tetraphosphonate materials: Synthesis, photocatalytic activity and heavy metal ion adsorption. *Microporous Mesoporous Mater.* **123** 234; (e) Hutchings G J 2004 Vanadium phosphate: a new look at the active components of catalysts for the oxidation of butane to maleic anhydride. *J. Mater. Chem.* **14** 3385
4. (a) Padhi A, Nanjundaswamy K, Masquelier C, Okada S, Goodenough J 1997 Effect of structure on the Fe3+/Fe2+ redox couple in iron phosphates. *J. Electrochem. Soc.* **144** 1609; (b) Qian L, Xia Y, Zhang W, Huang H, Gan Y, Zeng H, Tao X 2012 Electrochemical synthesis of mesoporous $FePO_4$ nanoparticles for fabricating high performance $LiFePO_4$/C cathode materials. *Microporous Mesoporous Mater.* **152** 128
5. (a) Kononova S, Nesmeyanova M 2002 Phosphonates and their degradation by microorganisms. *Biochemistry (Moscow)* **67** 184; (b) Kim T-W, Chung P-W, Slowing I I, Tsunoda M, Yeung E S, Lin V S-Y 2008 Structurally ordered mesoporous carbon nanoparticles as transmembrane delivery vehicle in human cancer cells. *Nano Lett.* **8** 3724
6. (a) Galownia J, Martin J, Davis M E 2006 Aluminophosphate-based, microporous materials for blood clotting. *Microporous Mesoporous Mater.* **92** 61; (b) Cote A P, Benin A I, Ockwig N W, O'keeffe M, Matzger A J, Yaghi O M 2005 Porous, crystalline, covalent organic frameworks. *Science* **310** 1166
7. (a) Gupta S K, Kalita A C, Dar A A, Sen S, Patwari G N, Murugavel R 2017 Elusive double-eight-ring zeolitic secondary building unit. *J. Am. Chem. Soc.* **139** 59; (b) Wilson S T, Lok B M, Flanigen E M 1982 Crystalline metallophosphate compositions. Google Patents
8. (a) Jensen T, Hazell R, Christensen A N, Hanson J 2002 Hydrothermal synthesis of lithium zinc phosphates: structural investigation of twinned α-$Li_4Zn(PO_4)_2$ and a high temperature polymorph β-$Li_4Zn(PO_4)_2$. *J. Solid State Chem.* **166** 341; (b) Cheetham A K, Férey G, Loiseau T 1999 Open-framework inorganic materials. *Angew. Chem. Int. Ed.* **38** 3268; (c) Rao C N R, Natarajan S, Choudhury A, Neeraj S, Ayi A A 2001 Aufbau principle of complex open-framework structures of metal phosphates with different dimensionalities. *Acc Chem Res* **34** 80; (e) Finn R C, Zubieta J, Haushalter R C 2003 Crystal chemistry of organically templated vanadium. *Prog. Inorg. Chem.* **51** 421
9. (a) Murugavel R, Choudhury A, Walawalkar M G, Pothiraja R, Rao C N R 2008 Metal complexes of organophosphate esters and open-framework metal phosphates: synthesis, structure, transformations, and

applications. *Chem. Rev.* **108** 3549; (b) Dar A A, Sharma S K, Murugavel R 2015 Is single-4-ring the most basic but elusive secondary building unit that transforms to larger structures in zinc phosphate chemistry? *Inorg. Chem.* **54** 4882; (c) Dar A A, Sen S, Gupta S K, Patwari G N, Murugavel R 2015 Octanuclear zinc phosphates with hitherto unknown cluster architectures: ancillary ligand and solvent assisted structural transformations thereof. *Inorg. Chem.* **54** 9458; (d) Dar A A, Bhat G A, Murugavel R 2016 Dimensionality alteration and intra-versus inter-SBU void encapsulation in zinc phosphate frameworks. *Inorg. Chem.* **55** 5180

10. (a) Yang Y, Pinkas J, Noltemeyer M, Schmidt H G, Roesky H W 1999 $[Zn_2(thf)_2(EtZn)_6Zn_4$ (μ4-O)$(tBuPO3)_8]$: A dodecanuclear zincophosphonate aggregate with a Zn_4(μ4-O) Core. *Angew. Chem. Int. Ed.* **38** 664; (b) Murugavel R, Kuppuswamy S, Gogoi N, Steiner A 2010 Assembling discrete D4R zeolite SBUs through noncovalent interactions. 3.(1) Mediation by butanols and 1, 2-bis (dimethylamino) ethane. *Inorg. Chem*. **49** 2153; (c) Murugavel R, Gogoi N, Suresh K G, Layek S, Verma H C 2009 Nuclearity control in molecular iron phosphates through choice of iron precursors and ancillary ligands. *Chem. Asian J.* **4** 923; (d) Murugavel R, Kuppuswamy S, Maity A N, Singh M P 2009 Di-, tri-, tetra-, and hexanuclear copper(II) mono-organophosphates: structure and nuclearity dependence on the choice of phosphorus substituents and auxiliary N-donor ligands. *Inorg. Chem.* **48** 183; (f) Murugavel R, Kuppuswamy S, Gogoi N, Boomishankar R, Steiner A 2010 Noncovalent synthesis of hierarchical zinc phosphates from a single $Zn_4O_{12}P_4$ double-four-ring building block: dimensionality control through the choice of auxiliary ligands. *Chem. Eur. J.* **16** 994
11. (a) Mason M R, Perkins A M, Matthews R M, Fisher J D, Mashuta M S, Vij A 1998 Synthesis and characterization of dimeric, trimeric, and tetrameric gallophosphonates and gallophosphates. *Inorg. Chem.* **37** 3734; (b) Walawalkar M G, Roesky H W, Murugavel R 1999 Molecular phosphonate cages: model compounds and starting materials for phosphate materials. *Acc. Chem. Res.* **32** 117
12. (a) Gupta S K, Rajeshkumar T, Rajaraman G, Murugavel R 2016 An air-stable Dy(iii) single-ion magnet with high anisotropy barrier and blocking temperature. *Chemical Science* **7** 5181, (b) Kalita A C, Gupta S K, Murugavel R 2016 A solvent switch for the stabilization of multiple hemiacetals on an inorganic platform: role of supramolecular interactions. *Chem. Eur. J.* **22** 6863; (c) Gupta S K, Dar A A, Rajeshkumar T, Kuppuswamy S, Langley S K, Murray K S, Rajaraman G, Murugavel R 2015 Discrete {Gd III 4 M}(M= Gd III or Co II) pentanuclear complexes: a new class of metal-organophosphate molecular coolers. *Dalton Transactions* **44** 5961; (d) Murugavel R, Sathiyendiran M, Pothiraja R, Walawalkar M G, Mallah T, Riviére E 2004 Monomeric, tetrameric, and polymeric copper di-tert-butyl phosphate complexes containing pyridine ancillary ligands†,⊥. *Inorg. Chem.* **43** 945; (e) Murugavel R, Sathiyendiran M, Pothiraja R, Butcher R J 2003 O–H Bond elongation in co-ordinated water through intramolecular P [double bond, length as m-dash] O··· H–O bonding.'Snap-shots' in phosphate ester hydrolysis. *Chem. Commun.* 2546
13. (a) Feng H, Zhou X-P, Wu T, Li D, Yin Y-G, Ng S W 2006 Hydrothermal synthesis of copper complexes of 4′-pyridyl terpyridine: From discrete monomer to zigzag chain polymer. *Inorganica Chim. Acta* **359** 4027; (b) Glasson C R, Lindoy L F, Meehan G V 2008 Recent developments in the d-block metallo-supramolecular chemistry of polypyridyls. *Coord. Chem. Rev.* **252** 940; (c) Housecroft C E 2014 4, 2′: 6′, 4′′-Terpyridines: diverging and diverse building blocks in coordination polymers and metallomacrocycles. *Dalton trans.* **43** 6594; (d) Zhang J, Su C-Y 2013 Metal-organic gels: from discrete metallogelators to coordination polymers. *Coordination Chemistry Reviews* **257** 1373; (e) Yang P, Wang M-S, Shen J-J, Li M-X, Wang Z-X, Shao M, He X 2014 Seven novel coordination polymers constructed by rigid 4-(4-carboxyphenyl)-terpyridine ligands: synthesis, structural diversity, luminescence and magnetic properties. *Dalton Transactions* **43** 1460, (f) Zhang G, Liu E, Yang C, Li L, Golen J A, Rheingold A L 2015 Copper (II) Complexes of 2, 2′: 6′, 2 ″-Terpyridine derivatives for catalytic aerobic alcohol oxidations–observation of mixed-valence CuICuII assembles. *Eur. J. Inorg. Chem.* **2015** 939
14. (a) Petitjean A, Xing L, Wang R 2010 Functional formamidines: pyridine substituents make an exception in the usual doubly hydrogen-bonded formamidine dimer. *Cryst. Eng. Comm.* **12** 1397; (b) Beves J E, Constable E C, Housecroft C E, Neuburger M, Schaffner S 2008 A one-dimensional copper (II) coordination polymer containing [Fe (pytpy) 2] 2+(pytpy= 4′-(4-pyridyl)-2, 2′: 6′, 2 ″-terpyridine) as an expanded 4, 4′-bipyridine ligand: a hydrogen-bonded network penetrated by rod-like polymers. *CrystEngComm* **10** 344; (c) Sun S-S, Lees A J 2001 Self-assembly organometallic squares with terpyridyl metal complexes as bridging ligands. *Inorganic chemistry* **40** 3154
15. Lv H, Rudd J A, Zhuk P F, Lee J Y, Constable E C, Housecroft C E, Hill C L, Musaev D G, Geletii Y V 2013 Bis (4′-(4-pyridyl)-2, 2′: 6′, 2′′-terpyridine) ruthenium (ii) complexes and their N-alkylated derivatives in catalytic light-driven water oxidation. *RSC Adv.* **3** 20647
16. (a) Constable E C, Zhang G, Housecroft C E, Neuburger M, Zampese J A 2009 Adding the second dimension with cadmium: two-dimensional sheets assembled from cadmium (ii) and 4′-phenyl-4, 2′: 6′, 4′′-terpyridine and locked by π-stacked interactions. *Cryst. Eng. Comm.* **11** 2279; (b) Constable E C 2007 2,2′:6′,2′′-Terpyridines: from chemical obscurity to common supramolecular motifs. *Chem. Soc. Rev.* **36** 246; (c) Zhang W-Y, Han Y-F, Weng L-H, Jin G-X 2014 Synthesis, characterization, and properties of half-sandwich iridium/rhodium-based metallarectangles. *Organometallics* **33** 3091
17. (a) Murugavel R, Kuppuswamy S 2006 Octameric and decameric aluminophosphates. *Angew. Chem. Int. Ed.* **45** 7022; (b) Murugavel R, Kuppuswamy S 2008 Organic-soluble tri-, tetra-, and pentanuclear titanium

(IV) phosphates. *Inorg Chem* **47** 7686; (c) Murugavel R, Kuppuswamy S, Gogoi N, Steiner A, Bacsa J, Boomishankar R, Suresh K G 2009 Controlling the structure of manganese(II) phosphates by the choice and ratio of organophosphate and auxiliary ligands. *Chem. Asian J.* **4** 143; (d) Murugavel R, Kuppuswamy S, Maity A N, Singh M P 2009 Di-, tri-, tetra-, and hexanuclear copper(II) mono-organophosphates: structure and nuclearity dependence on the choice of phosphorus substituents and auxiliary N-donor ligands. *Inorg. Chem.* **48** 183

18. (a) Bhat G A, Maqbool R, Dar A A, Ul Hussain M, Murugavel R 2017 Selective formation of discrete versus polymeric copper organophosphates: DNA cleavage and cytotoxic activity. *Dalton Trans.* **46** 13409; (b) Bhat G A, Maqbool R, Murugavel R 2018 Synthesis, characterisation, nuclease and cytotoxic activity of phosphate-free and phosphate-containing copper 4′-(N-methylpyridinium)-2,2′:6′,2″ terpyridine complexes. *J. Chem. Sci.* **130,** 21
19. Bhat G A, Rajendran A, Murugavel R 2018 Dinuclear manganese(II), cobalt(II), and nickel(II) aryl phosphates incorporating 4′-chloro-2,2′:6′,2″-terpyridine coligands - efficient catalysts for alcohol oxidation. *Eur. J. Inorg. Chem*. **2018** 795
20. Song J, Wang B-C, Hu H-M, Gou L, Wu Q-R, Yang X-L, Shangguan Y-Q, Dong F-X, Xue G-L 2011 In situ hydrothermal syntheses, crystal structures and luminescent properties of two novel zinc (II) coordination polymers based on tetrapyridyl ligand. *Inorganica Chim. Acta* **366** 134
21. Kosolapoff G M, Arpke C K, Lamb R W, Reich H 1968 Structural effects in reactions of organophosphorus compounds. I. Reactions of phosphorus oxychloride with hindered phenols. *J. Chem. Soc. C: Organic* 815
22. Dar A A, Mallick A, Murugavel R 2015 Synthetic strategies to achieve further-functionalised monoaryl phosphate primary building units: crystal structures and solid-state aggregation behavior. *New. J. Chem.* **39** 1186
23. Farrugia L 1999 WinGX suite for small-molecule single-crystal crystallography. *J. Appl. Crystallogr*. **32** 837
24. Altomare A, Cascarano G, Giacovazzo C, Guagliardi A 1993 Completion and refinement of crystal structures with SIR92. *J. Appl. Crystallogr.* **26** 343
25. Sheldrick G M 2015 Crystal structure refinement with SHELXL. *Acta Cryst. C.* **71** 3
26. Murugavel R, Sathiyendiran M, Walawalkar M G 2001 Di-tert-butyl phosphate complexes of cobalt (II) and zinc(II) as precursors for ceramic $M(PO_3)_2$ and $M_2P_2O_7$ materials: synthesis, spectral characterization, structural studies, and role of auxiliary ligands. *Inorg. Chem.* **40** 427
27. Lugmair C G, Tilley T D, Rheingold A L 1997 Zinc di (tert-butyl) phosphate complexes as precursors to zinc phosphates. manipulation of zincophosphate structures. *Chem. Mater.* **9** 339
28. Ma Z, Wei L, Alegria E C, Martins L M, da Silva M F C G, Pombeiro A J 2014 Synthesis and characterization of copper (ii) 4′-phenyl-terpyridine compounds and catalytic application for aerobic oxidation of benzylic alcohols. *Dalton Trans.* **43** 4048
29. Momeni B Z, Heydari S 2015 Design of novel copper (II) and zinc (II) coordination polymers based on the 4′-functionalized terpyridines. *Polyhedron* **97** 94